ECS Transactions, 3 (13) 37-49 (2007)
10.1149/1.2721429, copyright The Electrochemical Society

Electrochemical Measurements in Cement Extract Solutions on Reinforcing Steel, Previously Conditioned in Concrete

D.A.Koleva[a], J.H.W.de Wit[b], K.van Breugel[a], V.Bachvarov[c], H.Kolev[d], A.Fraaij[1]

[a]Delft University of Technology, Faculty of Civil Engineering and Geosciences, Section CT Material Science, Stevinweg 1, 2628 CN Delft, Netherlands
[b]Delft University of Technology, Faculty 3mE, Department Material Science and Engineering, Mekelweg 2, 2628 CD Delft, Netherlands
[c,d]Bulgarian Academy of Sciences, [c]Institute Physical Chemistry, [d]Institute of Catalysis, Acad. G. Bonchev, bl. 11, Sofia 1000, Bulgaria

The corrosion behavior of reinforcing steel, previously embedded in concrete and maintained in conditions of corrosion and two regimes (conventional and pulse) of cathodic protection (CP), was characterized using electrochemical measurements in cement extract (CE) solutions of pH 12.6. The investigation aimed at determination of the properties of the product layers, *previously formed* on the steel surface. The study further allowed evaluation of the CP effectiveness in terms of steel surface oxidation/reduction behavior in the alkaline medium of CE. Based on the similar electrochemical behavior of protected specimens, it can be concluded that the pulse CP is as effective as the conventional CP regime. Moreover, the surface film, formed in pulse CP conditions appears to be more homogeneous and resistive, compared to the conventional CP regime.

Introduction

It is known that the product layers on the steel surface in $Ca(OH)_2$ environment (as in concrete or cement extract) are composed of several layers and in the simplest case are being considered as inner and strongly adherent formation, with composition similar to Fe_3O_4 and a gelatinous layer of iron hydroxides, where Fe^{2+}/Fe^{3+} can be detected [1-3]. Calcium ions can be incorporated in the outer atom layers of the inner layer and increase the protective ability of the product layers when no chlorides are present [3]. Similar effects are attributed to the presence of Si, which is about 21 w.% in Portland cement in the form of SiO_2. Adding SiO_2 to model pore solutions with pH ~10-13, is found to promote a more protective film, probably due to its incorporation in the film [4, 5].

The passive layer formation (as in non-corroding conditions) or the passive layer breakdown and further development of a thicker and non-homogenous product layer (as in corroding conditions) are mechanisms which already differ form the case of product layers transformations when cathodic protection is applied. The conventional basis for impressed current CP relies on inducing a negative steel potential shift [6] i.e. more cathodic than -850 mV SCE, where corrosion is thermodynamically restricted [7]. In addition to the negative potential shift, the cathodic current induces changes of the local environment in the vicinity of the steel surface, rendering it less aggressive to steel and hence promoting “healing” of the steel surface [8, 9].

There are several aspects that one should take into consideration when evaluating electrochemical performance of systems as in the present study in terms of product layers formation and performance: One aspect is the substitution of iron oxides/hydroxides layers with calcium and/or silica. This would cause structural changes in the oxide/hydroxide layers and will probably lead to different catalytic activity [10]. Second aspect is the thickness, morphology and adhesion of the product layers. Previous studies of the authors [11] reveal that protected specimens at 270 days of age, exhibit a thinner layer, composed of mainly Fe_3O_4, in contrast to a multi-layered, thicker product formation for the corroding surfaces. The former layers are characterized with higher compactness, whereas the latter are composed of non-adherent compounds as akaganeite (β-FeOOH.Cl_2) and predominance of goethite (α-FeOOH) and lepidocrocite (γ-FeOOH). These observations are consistent with reported results from similar research [3], where the presence of α- and γ-FeOOH are detected in the outer product layers, and Fe_3O_4 and α-FeOOH in the inner layers. In addition to this sequence, β-FeOOH.Cl_2, being a needle shape formation at earlier age or bundles of rods of hollow subcrystals at later ages, is non-adherent compound, which does not accommodate in the product layer.

By performing this study in CE solution, as model concrete pore solution, we aimed at comparative investigation of the naturally formed (during steel embedment in concrete) product layers on reinforcing steel after 460 days of initial conditioning i.e. previous corroding, CP, pulse CP and non-corroding conditions, rather than studying any further passivation of the steel electrodes in contact with the CE solution. Thus, after CP applications, the product layers on the previously corroding steel surface were expected to have different performance, compared to non-corroding and corroding conditions, providing supporting evidence for the efficiency of the CP techniques.

Experimental materials and methods

Materials

The samples for the present investigation were prepared by cutting cylinders (h=15 mm, d=6 mm) from the previously (for 460 days) embedded and conditioned in concrete reinforcing steel (specimen set-up and details for embedded conditions are reported in [11]). The steel, initially cast in concrete “as received”, was construction steel FeB500HKN (ribbed bars, d=12mm, C < 0.12 w.%).

The samples comprise three main groups: samples from a previously corroding group reinforced cylinders (denoted as C), samples from a non-corroding (or reference) group reinforced cylinders (denoted as R) and samples from a previously protected group cylinders (denoted as P). Group P comprises 4 subgroups: P1a and P2a are specimens which were previously under CP and pulse CP, using current density of 5 mA/m^2 steel surface, applied at 60 days of age. Groups P1b and P2b are specimens, initially maintained under CP and pulse CP, but using higher current density – 20 mA/m^2 , CP both regimes being applied at 150 days of age. The pulse regime for all pulse CP protected specimens used duty cycle of 12.5 to 50 % at 1 kHz frequency i.e the effective CP current density in case of pulse CP was always 50% of the CP current density in the relevant conventional CP regime.

The top and bottom cross sections of the so received steel samples were isolated (thus working area for the electrode was only the outer surface of the bar, previously exposed in the different technical conditions, while being embedded in the concrete) and used as working electrodes in a common 3-electrode cell arrangement; the working electrolyte

was CE solution of pH 12.6, prepared from ordinary Portland cement OPC CEM I 32.5R (the same cement type, used previously for the concrete mixture), reference electrode was a saturated calomel electrode (SCE), counter electrode was a cylindrical Pt mesh (positioned around the working electrode).

Methods

Electrochemical methods: electrochemical impedance spectroscopy (EIS) and normal staircase cyclic voltammetry (CVA) were performed for all investigated specimens in CE solution, at room temperature and after allowing for OCP stabilization before each measurement (~ 40 min). The EIS measurements were carried out in the frequency range of 50 kHz to 10 mHz by superimposing an AC voltage of 10 mV. CVA was carried out at 200 mV/s scan rate, starting at -1.6 V and first vertex potential of 0.9 V (SCE). The used equipment was EcoChemie Autolab - Potentiostat PGSTAT30, combined with FRA2 module, using GPES and FRA interface.

X-ray diffraction (XRD) measurements were performed by scanning representative areas of about 1 cm2 (directly on the surface) of the test specimens, using D8 Advance Diffractometer,"Bruker AXS". A Vantec position sensitive detector (window 6 deg.) was used for detection. Energy source was CoKα (1.789A) and the tube settings were 45kV and 35mA.

X-ray photoelectron spectroscopy (XPS) measurements were carried out using ESCALAB MkII (VG Scientific) electron spectrometer at a base pressure in the analysis chamber of $5x10^{-10}$ mbar (during the measurement $1x10^{-8}$ mbar). The photoelectrons were excited using AlKα X-ray source (excitation energy hν=1486.6 eV). The pass energy of the hemispherical analyzer was 20 eV (for Fe 2p – 50 eV), 6 mm slit widths (entrance and exit). The instrumental resolution measured as the full -width at a half-maximum (FWHM) of the $Ag3d_{5/2}$, photoelectron peak is 1 eV. The energy scale is corrected to the C1s - peak maxima at 285 eV for electrostatic charging.

SEM and EDAX investigations were performed with environmental SEM, ESEM Philips XL30, equipped with secondary, backscatter electron and large field detectors, operating at accelerating voltage of 20 to 25 kV for imaging. For EDAX analysis and composition of the product layers, directly on the steel surface, 7 to 15 kV was used. The results on morphology and composition of product layers at 460 days of age were consistent with observations for 270 days of age, reported in [11].

Results and discussion

Surface analysis – XPS.

The surface composition of the product layers, initially formed on the steel surface while the reinforcement was in embedded conditions i.e. prior to the electrochemical measurements in CE solution, was investigated by XPS and XRD techniques (measurements were performed on representative areas of 1 cm^2 steel surface). Fig. 1 depicts the survey XPS scan, the analyzer resolution was 0.45eV(1eV), which gives a total instrumental resolution (as measured with the FWHM of Ag (3d photoelectron line) of 1.06 (1.75) and 1.18 (1.8) eV for MgKα and AIKα excitation sources respectively. The survey scan reveals the presence of principal peaks for Fe and O (as metal oxides/hydroxides), Ca and Si, incorporated from the cement paste as substitutions in the products layers, Na and Cl (present as consequence of experimental environment,

relevant to the initial conditioning of the specimens), Cl being detectable for corroding specimen C and for one of the specimens from group P1a (conventional CP).

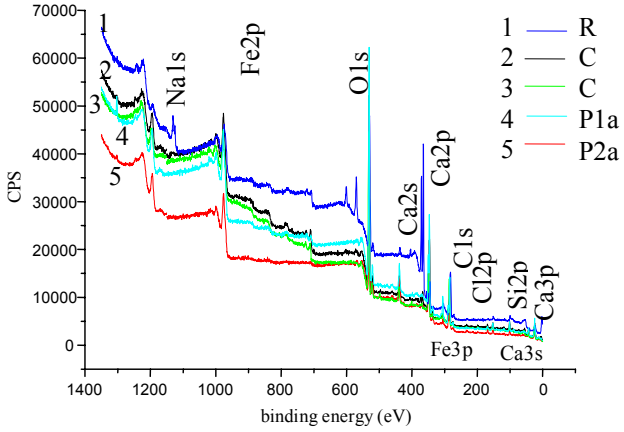

Fig.1 Survey XPS scans for the investigated steel samples before electrochemical measurements in CE solution: Na1s; Fe2p,3p; O1s; Ca2s,2p,3p,3s; Cl2p; C1s; Si2p.

Surface analysis – XRD.

The peak intensity in the XRD diffractograms is generally corresponding to the amount of specific corrosion products, thus allowing a qualitative comparison between different specimens. Fig. 2 shows the XRD patterns (using CoKα radiation) for two corroding (C) specimens (460 days of age) and protected specimen (P2a, pulse CP, 460 days of age).

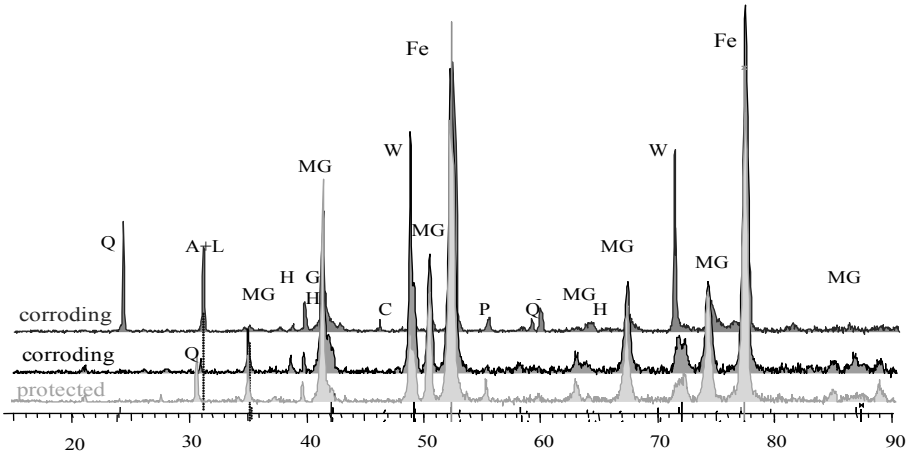

Fig.2 X-ray diffraction patterns for corroding specimens (group C) and protected specimen P2a (b), using CoKα radiation: C- calcite, G- goethite, MG – magnetite, L – lepidocrocite, Q – quartz, W – wustite, Ar – aragonite, P – portlandite, A – akaganeite, H – hematite

In general the XRD patterns for the corroding specimens reveal sharper peaks for low valent oxides (e.g. wustite –W) and shallower peaks for magnetite (MG). In addition, akaganeite (A) is identified only in the corroding specimens (at 2θ 31.2°), overlapping with the peak for lepidocrocite (L); goethite (G) and hematite (H) are detected at 2θ 39.5°, 64°. Contributions of Quartz - Q (SiO2) and Portlandite –P (Ca(OH)2) were detected

along with the iron oxides and hydroxides. Quartz (Q) is corresponding to sand grains; Portlandite (P) is both derived from relicts from the cement paste, or from the Ca-rich layer adhered to the steel surface. The magnetite peaks at 2θ 35°, 41°, 50.5°, 62.5°, 67°,74° are sharper for the protected specimens, in contrast the peaks for wustite at 2θ 42.5°, 49.1°, 72.5° are more pronounced for the corroding specimen.

A layer, enriched in magnetite and hematite, as in the protected specimens, will have better performance in terms of adherence, compactness and homogeneity, whereas a layer composed from wustite, akaganeite, lepidocrocite (as in the corroding specimens) will have lower protective properties, lower adhesion (especially in the presence of akaganeite) and reduced corrosion resistance. Hence, CP brings about favorable modifications of the corrosion products in terms of higher amounts of protective and adhering to the steel surface Fe_3O_4, which along with the Ca-rich layer (evidenced by adhered portlandite) and non detectable by XRD oxy(hydroxy) chlorides, denote for the CP efficiency and supplies evidence for the fundamental reasons underlying the CP mechanisms as far as product layers formation and conversion are concerned.

Electrochemical measurements

The steel electrodes from each group (as previously defined: reference R, corroding C, protected P1a, P2a, P1b and P2b) were subject to electrochemical testing in CE solutions.

EIS measurements

Figs. 3 to 5 present the EIS response of the investigated specimens, after OCP stabilization in CE solution. The derived parameter was mainly polarization resistance (R_p), which can be associated with the corrosion process (the anodic oxidation of steel) as well as other electrochemical processes involving corrosion products, thus providing information for the overall reaction rates.

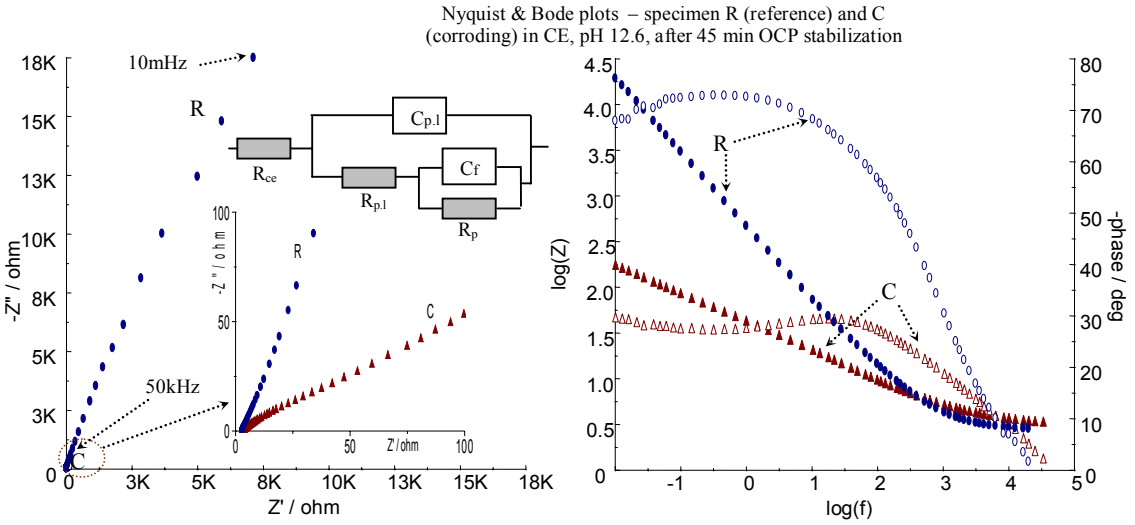

Fig.3 A comparison of impedance response for specimen group C (corroding) and R (reference) in CE solution (working electrode at 460 days of age) after OCP stabilization only.

Fig. 3 presents the impedance response in Nyquist (left) and Bode (right) formats for corroding specimen C and reference specimen R, and the used equivalent electrical circuit (incorporated in Fig.3,left). The elements of the equivalent circuit present the following physical meaning: R_{ce} is the CE resistance; the first time constant ($R_{p.l}$,$C_{p.l}$) is

attributed to resistance and properties of the product layers (or redox transformations in the product layers); the second time constant (R_p, C_f) deals with the electrochemical reaction on the steel surface.

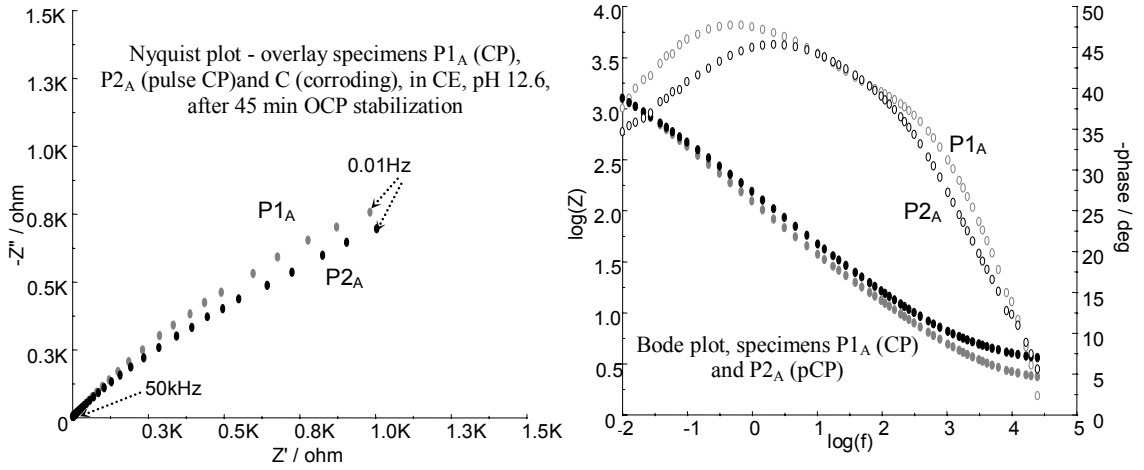

Fig. 4 A comparison of impedance response for protected cells P1a (CP) and P2a (pulse CP), (working electrode at 460 days of age, CP both regimes applied at 60 days of age) in CE solution, after OCP stabilization only.

Fig.4 depicts an overlay of the impedance response for the protected specimens P1a and P2a, which are steel samples from previously protected for 400 days reinforcing steel (CP both conventional (P1a) and pulse (P2a), was applied at 60 days of age, using CP current density of 5 mA/m^2).

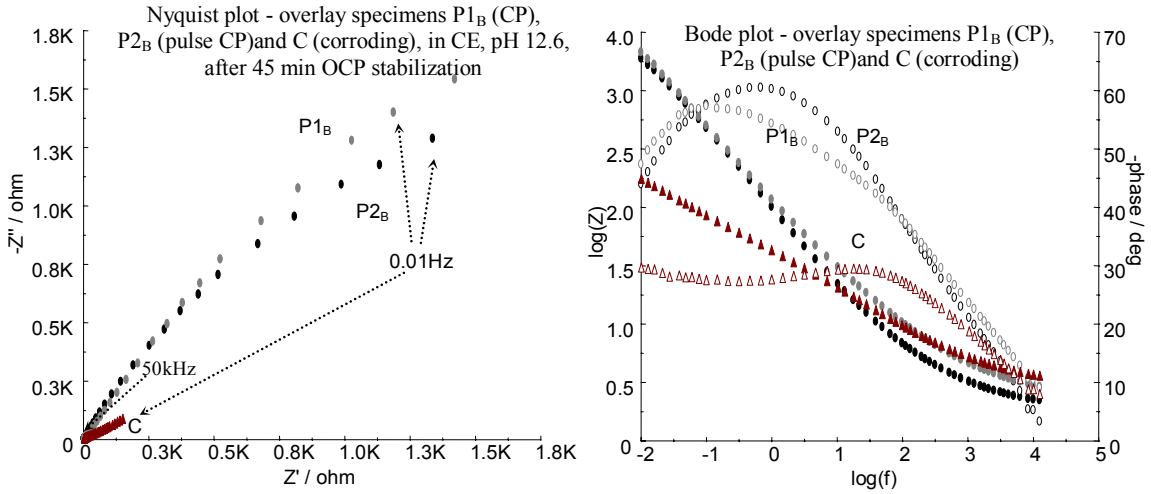

Fig. 5 Impedance response for protected cells P1b (CP) and P2b (pulse CP), (working electrode at 460 days of age, CP both regimes applied at 150 days of age) and comparison with the response for corroding specimen C at the same age, in CE solution, after OCP stabilization only.

The shape of the experimental curves and the recorded parameters after fitting procedures (Table 1) for specimens P1a and P2a (Fig.4) are very similar to those depicted on Fig. 5 for specimens P1b and P2b, which are steel samples from previously protected for 310 days reinforcing steel (CP both conventional (P1b) and pulse (P2b), was applied

at 150 days of age, using CP current density of 20 mA/m^2). The previously CP protected specimens (index "1") from all groups exhibit a slightly higher low frequency impedance limit, compared to the pulse CP protected specimens.

Table 1 Best fit parameters from EIS response in CE solution*

Specimen	$R_{p.l}$ *Ohm.cm^2*	$C_{p.l}$ *μF.cm^{-2}*	R_p *kOhm.cm^2*	C_f *μF.cm^{-2}*	E_{ocp} *mV(SCE)*
P1a	7.1	60	24.4	52	-502
P2a	25.9	48	20.9	23	-417
P1b	12.5	191	37.6	26	-480
P2b	5.2	184	27.7	50	-472
C	120	974	1.8	520	-573
R	8.5	39	363.5	42	-226

*R_{ce} for all specimens is approx. 3 Ohm (this is the CE solution resistance, varying between 2.8 and 3 Ohm, geometry of the cell and experimental set-up, as well as geometrical surface of all specimens is identical).

Fig.3 shows the significant difference of the impedance response for corroding (C) and non-corroding (R) specimens in the low frequency domain, attributed to accelerated corrosion state in the former and passive condition in the latter case. The C_f values for specimen R tend towards the values for $C_{p.l.}$ (42 μF.cm^{-2} and 39 μF.cm^{-2} respectively), which corresponds to the low rate of oxidation process for this specimen. The derived R_p for corroding specimen C is much lower compared to non-corroding and protected specimens (Table 1). The corresponding C_f is significantly higher (520 μF.cm^{-2}) compared to protected specimens P (23 to 52 μF.cm^{-2}), attributed to spreading the corrosion damage on a larger surface area. The $C_{p.l}$ values for all specimens are higher than C_f values and can be denoted to modifications in the structure of the product layers. The capacitance $C_{p.l}$ for corroding specimen C is highest among the investigated specimens, denoted to capacitance associated with redox processes of product layers containing chlorides (as in specimen C) and can be attributed to the easier oxidisability of the product layer in the presence of Cl^-. Furthermore, the protective properties of this product layer are low, evidenced by the low R_p values. In specimen C, $C_{p.l}$ and $R_{p.l}$ are significantly higher compared to the other conditions because in the presence of chlorides, the corrosion rate is initially high, thicker (but not protective) layers are quickly formed, thus high values of $R_{p.l}$ and $C_{p.l}$ can be observed even at earlier age. In contrast, the capacitance related to product layers ($C_{p.l}$) for specimens P and R is much lower, $R_{p.l}$ as well, which corresponds to thin layers of products and higher R_p values (lower corrosion rate).

Additionally, there is a larger surface area of the products, composing the surface layer in specimen C, contributing to the overall process (as reported by [12], the surface area in m^2/g decreases in the sequence of: $Fe_xOH_y.zH_2O$ > β-FeOOH.Cl_2 > α-FeOOH > α-Fe_2O_3). Along with the above considerations, another aspect is the conductivity (electron, ionic, electrical) of the formed layers. For example, electrical conductivity of goethite, hematite and magnetite is decreasing in the order: magnetite-hematite-geothite [13], which suggests that the layers containing mostly magnetite (as in specimens P) will exhibit lower limitations to current flow (as in the time of an electrochemical measurement, consequently lower $R_{p.l}$), while specimens with high amounts of goethite (oxy-hydroxides are in higher amounts in the corroding specimens as consequence of more oxygen supply via micro-cracks) will exhibit higher resistivity to current flow (higher values for $R_{p.l}$).

Comparing the impedance response for protected specimens and corroding specimen (Fig.5), it is obvious that the magnitude of impedance and the phase angles are higher for

all protected specimens, compared to specimen C, which denotes for effectively working CP in all previously maintained protected conditions and the formation of a more corrosion resistive film. The pulse CP (both regimes of lower and higher CP current density) is obviously at least as effective as the conventional CP technique, evidenced by the similar to conventional regimes EIS response.

Cyclic voltammetry.

Cyclic voltammetry is a useful method for investigating the mechanisms if surface oxidation/reduction behavior of steel in an alkaline environment, as the concrete pore solution, and as such has been extensively used in studying the performance of bare steel in model solutions [1,3,14,15,16-18].

A series of cyclic voltammograms (CVs) was acquired at steel samples from each technical condition (previously described groups C, R and all P groups) in CE solution, after allowing for OCP stabilization (~ 40 min). The stabilized electrode potentials varied between -220 mV SCE for specimens R to -570 mV SCE for specimen C, the groups P showed minor variation, stabilized OCP values were ~ 420 mV SCE. The different steel potentials in the CE solution (pH 12.6) are denoted to the different properties of the initially formed product layers. The scan rate for performing the CVA measurements was 200 mV/s, allowing for well distinctive peaks in the voltammograms, which was not the case at lower scan rates. When the scan rate was decreased from 100 to 20, 5 and 1 mV/s, the cathodic reduction peak shifts cathodically, while the anodic peaks practically disappear, the passive potential region becomes much extended and almost no other features can be easily observed. Hence, a scan rate of 200 mV/s was used in the present study, as also used in similar research [19].

Fig.6 depicts an overlay of the 1st (left) and the 15th (right) scans for all here investigated specimens. Figs.6 a)b) present an overlay for specimens R (reference) and all groups of protected specimens (P1a, P2a, P1b and P2b); Figs.6c)d) present a comparison of the 1st and 15th scans for corroding specimen C, reference specimen R and the couple of protected specimens, on which CP was applied at 60 days of age (P1a and P2a). The voltamogramms are obtained, as mentioned, at scan rate 200 mV/s after allowing for OCP stabilization (approx.40 min). The peaks II (-0.99V to -1.1V) and III (-0.6V to -0.5V) in the forward scan and peaks IV (approx. 0.51V) and V (approx. -1.25V) in the reverse scan are mainly distinguished (all potentials are vs SCE). As seen from the plots, with cycling the previously protected specimens (groups P) behave similarly to reference (previously non-corroding) conditions. The best performance in terms of product layer corrosion resistance with cycling is for specimen P2a, which is steel surface, previously pulse CP protected (pCP applied at 60 days of age). This is evidenced by the lowest cathodic and anodic currents with cycling in addition to the highest hydrogen and oxygen evolution overpotentials. In what follows, the main characteristics of the cyclic voltamograms will be discussed along with separate presentation of scan overlays for the different conditions.

Figs.7a)b) depict an overlay of 1st to 15th scans for specimens R and C, Figs.8,9 presents an overlay of CV scans for the couple of protected specimens P1b (conventional CP) and P2b (pulse CP).

For specimens R (Fig.7a) the anodic peak II reaches almost constant height after 2 to 5 cycles, while the second anodic peak (III), associated with the oxide film development, increases with increasing the number of cycles. The same observation holds for the

corresponding reduction peak V. Peak IV becomes more distinct after the 5th cycle, both reduction peaks achieving a stable height in the last few cycles.

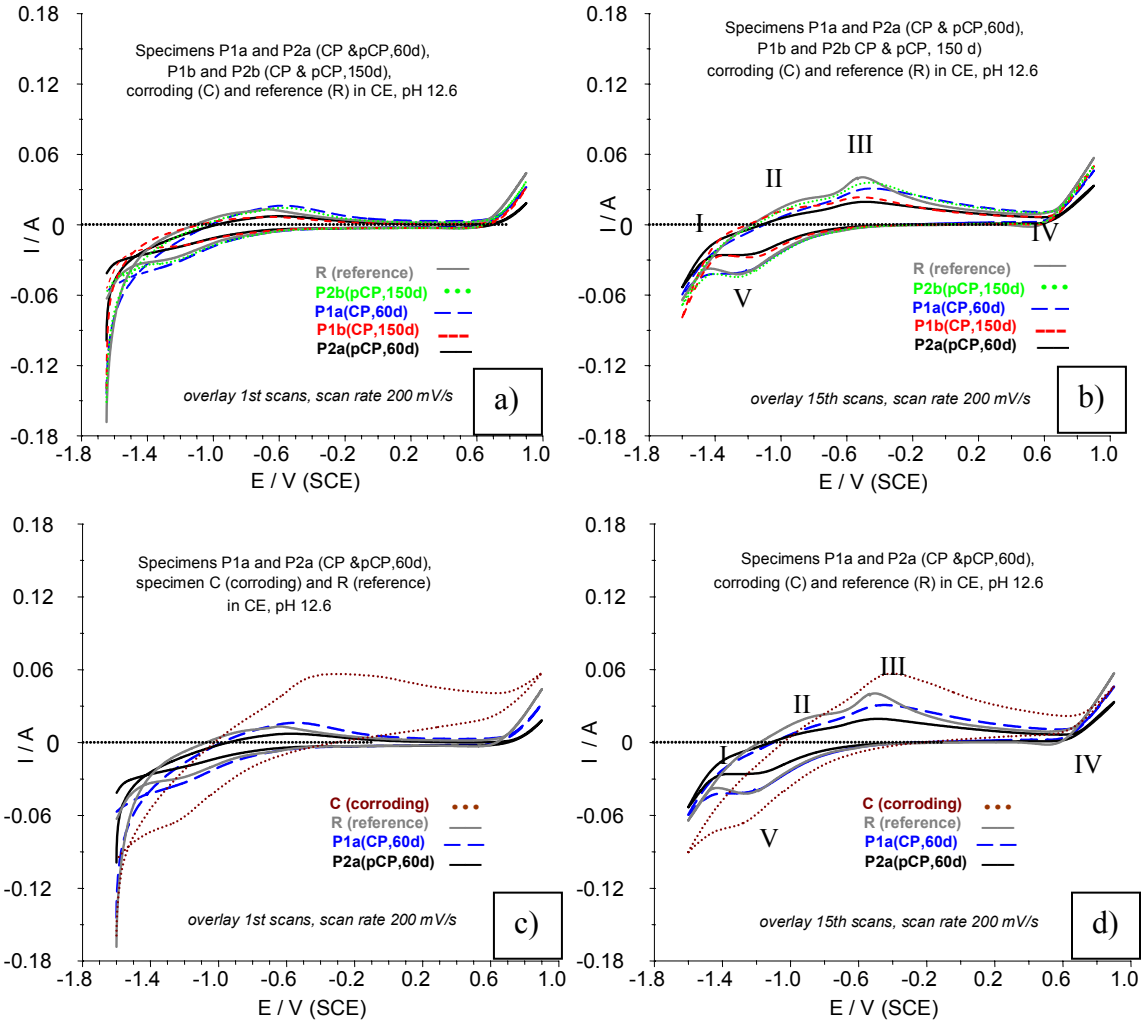

Fig. 6 (a,b) Overlay of the 1st and 15th scans for groups R and all P groups and (c,d) overlay of corroding group C with groups R, P1a and P2a (CP and pCP applied at 60 days)

Although the peak current densities at peaks III and V increase with cycling, the slope of the curves becomes stable after the 5th cycle and approaches relatively constant values i.e. there is a tendency to reach a steady state, as reported in similar research [16, 20]. In specimen C (which was previously corroding specimen) a shoulder peak (IIIa at about –300 mV) is observed (Fig.7b), denoted to a more active dissolution process in this specimen, which along with the strong distortion of the voltammogram, compared to the other specimens (Figs.6c)d),7b)), suggests a very low corrosion resistance of this film, evidenced by the high currents in the normally passive region at potentials anodic to peaks III and IIIa. After the 1st scan, there is a drop of the current in the region of peak IIIa, but almost no change is observed for the peak current III.

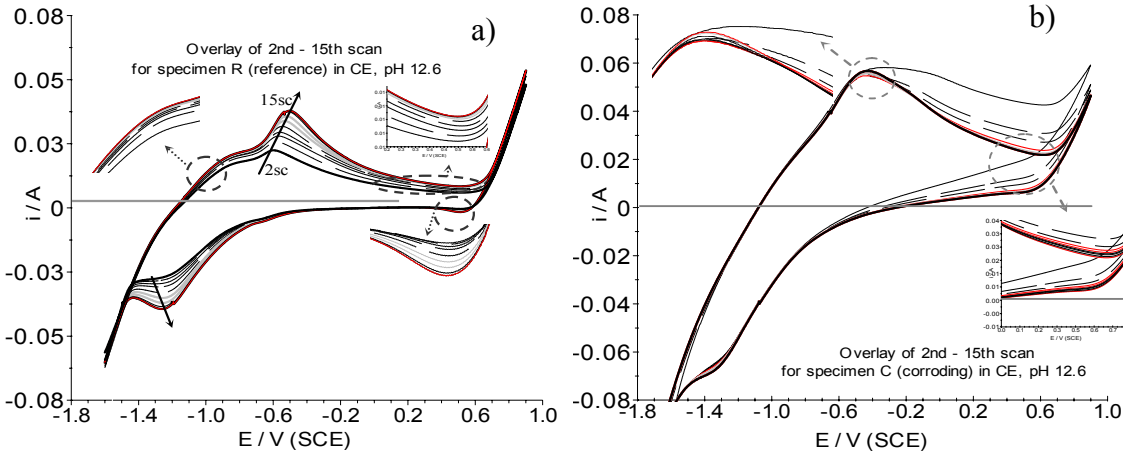

Fig.7 Overlay of the 1st to 15th scans for group R (a) and for group C (b) in CE solution, after OCP stabilization only.

In the region of peak IV, which for specimen C is anodic, a shift towards cathodic current is observed, but the peak remains in the anodic region till the 15th scan and further on with cycling (data not presented). After the 5th scan, the anodic current in the region -0.3V to 0.6 V again increases and reaches stable, significantly higher values, compared to specimens R. The observations could be probably attributed to some limitations in the beginning of cycling, related to rapid formation of corrosion products with larger surface area in the first scan, which is evidenced by the highly distorted curves and high currents. There are almost no limitations in the cathodic region of hydrogen evolution (region I), peak II is hardly distinguishable due to the very steep slope of the transition from peak II to peak III.

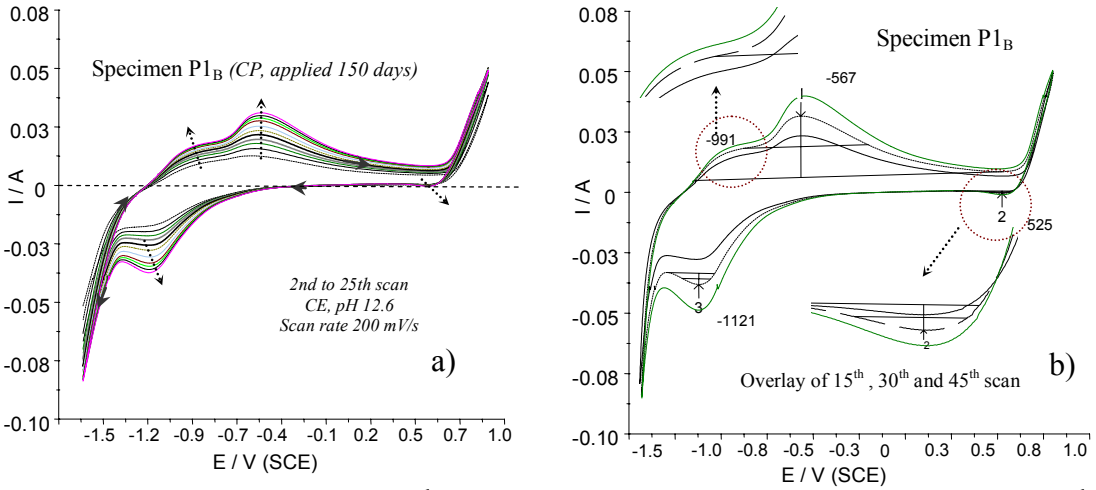

Fig.8 (a) Overlay of the 1st to 15th scans for group P1b (CP,150d); (b) overlay of 15th, 30th and 45th cycle for the same group, after OCP stabilization only.

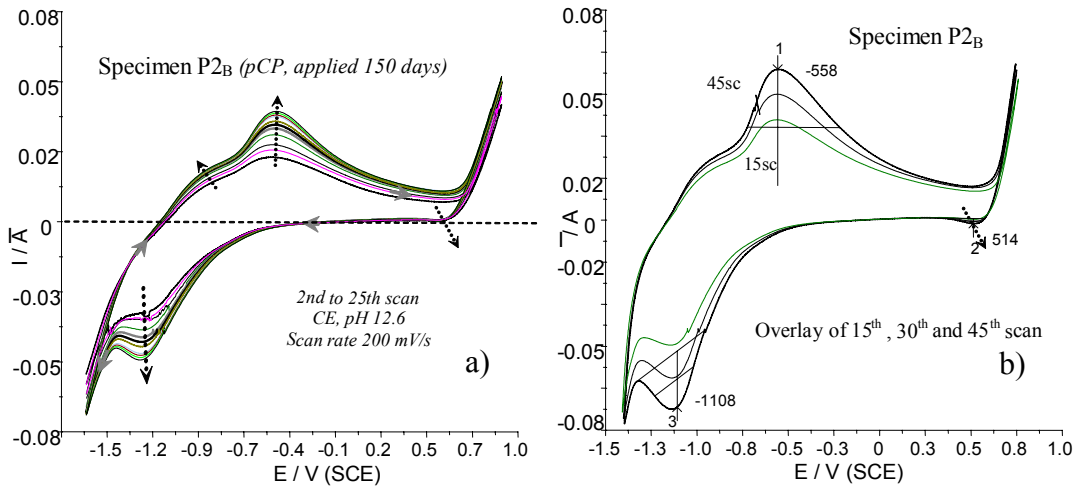

Fig.9 (a) Overlay of the 1st to 15th scans for group P2b (pCP,150d); (b) overlay of 15th, 30th and 45th cycle for the same group, after OCP stabilization only

The overlay of 1st to 15th scans for both groups P (Figs 8a and 9a) shows similar behavior and peak current ranges as for the reference specimen R (Fig 6a) i.e. a tendency to reach a steady state with cycling and change of peak currents height, denoted to thickening of the oxide layer. Moreover, an increase in the peak current only, not accompanied by anodic shift of the peak potential (as observed for specimens R, Fig.6a), suggests that the product layer in the protected specimens is more homogeneous and compact.

These observations are supported by further cycling (from 15th to 45th cycles), depicted on Figs. 8b) and 9b), showing almost constant values of anodic and cathodic currents in the potential region of 0V to 0.6V, which again is consistent with the observations in specimen R.

Relevant to all investigated specimens are the anodic/cathodic reactions, as summarized below [21, 22], corresponding to the observed peaks.

Region I – hydrogen evolution reaction
Peak II (approx.-990mV): $Fe + 2OH^- = Fe(OH)_2 + 2e$
Peak III (approx.-554mV):
$Fe(OH)_2+OH-=[Fe(OOH)] + H_2O + e$,
followed by a chemical reaction of:
$2[Fe(OOH)] = [Fe_2O_3.H2O]$

Peak IV (approx.510mV): poorly defined, formation of calcium substituted layers [10].
Peak V (approx.-1250mV): $FeOOH \rightarrow Fe(OH)_2$; $Fe_3O_4 \rightarrow Fe(OH)_2$

Although the electrochemical reactions, corresponding to the various peaks in alkaline solutions have been discussed and reported by previous investigations [e.g. 23–29], they have not been strictly identified. There is a general agreement however, which is as follows: Peak II is generally attributed to steel dissolution i.e. to the formation of ferrous hydroxide from the base steel surface. The current densities at peak III are characteristic of the onset of passivation, at which point Fe^{2+} is being oxidized to insoluble Fe^{3+}. This peak is associated with the transformations in the outer hydrous oxide layer and the relatively intact inner anhydrous oxide layer. At peak III, the increasing rate of oxidation to insoluble Fe^{3+}, or possibly substituted layer of $CaFe_2O_4$ [20, 23] is further overtaken by the increasing impermeability of the passivating layer. Hence

the properties in terms of compactness, permeability, corrosion resistance of the product layers at potentials anodic to peak III are determined by the current densities in this region.

Conclusions

The similar electrochemical behavior of all protected specimens denotes that the pulse CP is as effective as the conventional CP regime. Moreover, the surface film, formed in pulse CP conditions appears to be more homogeneous and resistive, compared to the conventional CP regime. The specimens, on which pulse CP was applied at 60 days of age, exhibit the best performance with external polarization and cycling in CE. The observation suggests that pulse CP, using 50 % of the current density applied in the relevant CP regime, is sufficient for cathodic protection in reinforced concrete, subjected to chloride ingress. Further, CP and pulse CP using higher current densities (20 mA/m^2) but applied on later stage of 150 days (which suggests relatively higher corrosion rates in these specimens before protection), lead to similar results in terms of electrochemical behavior of the steel electrodes. However, pulse CP applied at 150 days does not show better performance compared to the relevant conventional regime, as it was found for pulse CP applied at 60 days of age.

Exposure to CE for longer periods does not result in increased corrosion resistance i.e. the initially formed films on the surface of protected specimens are with good performance and better properties. The product layers on the steel surface of the previously corroding specimens are difficult to repair, even after longer periods of exposure to CE of pH 12.6.

References

1. O. A. Albani, J. O. Zerbino, J. R. Vilche, A. J. Arvia, *Electrochim.Acta*, **31**, 1403 (1986)
2. D. S. Leek, A. B. Poole in: Page C.L., Treadway K.W, Bamforth P.B., Eds: Proceedings of the 3rd International Sypmosium on Corrosion in Reinforced Concrete, London, *Elsevier Appl.Sci*, **67** (1990)
3. H. Oranowska, Z. Szklarska-Smialowska, *Corros.Sci*.,**21**, 735 (1981)
4. S. T. Amaral and I. L. Muller, *Corros.Sci*., **41**, 747 (1999)
5. S. T. Amaral and I. L. Muller, *Corros.Sci*., **41** , 759 (1999)
6. J. Bennett, T. Turk, "Technical alert – criteria for the CP applied to reinforced concrete bridge elements", Report No SHRP-S-359, SHRP, Washington D.C. (1994)
7. M. Pourbaix, Atlas of Electrochemical Equilibria in aqueous solutions, *NACE*, 312, (1996)
8. G. K. Glass, W. K. Green, J. R. Chadwick, "Long term performance of CP systems in reinforced concrete structures", Proceedings of *Corrosion 91*, **3**, Institute of Corrosion, Leighton Buzzard, UK (1991)
9. G. K. Glass, *Corros.Sci*., **26**, 441 (1986).
10. C. Andrade, M. Keddam, X. R. Nóvoa, M. C. Pérez, C. M. Rangel and H. Takenouti, *El.Acta*, **46**, 3905(2001)

11. D.A. Koleva, J. H. W.de Wit, K. van Breugel, Z.F. Lodhi, E. van Westing, *Investigation of corrosion and CP in reinforced concrete. Part I: Application of electrochemical techniques*. submitted to *J.Electrochem.Soc*., July 2006.
12. S.E.O'Reilly, M.F. Hochella, *Geochim.&Cosmochim.Acta*, **67**, 4471 (2003).
13. N. Guskos, *Mater.Research Bulletin*, **37**, 1051 (2002).
14. T. Zakroczymski, C. J. Fan, Z. Szklarska-Smialowska, *J.Electrochem.Soc* **132** (1985)
15. M. F. Montemor, A. M. P.Simoes, M. G. S.Ferreira, *Corrosion***, 54**, 347 (1998)
16. P. Gu, Y. Fu, P. Xie, J. J. Beaudoin, *Cem.Concr.Comp*., **24**, 38 (1994)
17. J. L. Dawson, P. E. Langford In: P. E. Francis and T. S. Lee (Eds), ASTM STP-970, ASTM International, Philadelphia, 264 (1988)
18. C. Andrade, V. M. Blanco, A. Collazo, M. Keddam, X. R. Novoa, H. Takenoutti, *El.Acta*, **44**, 4313 (1999)
19. L. Veleva, M. A. Alpuche-Aviles, M. K. Graves-Brook, D. O. Wipf, *J.Electroanal.Chem*., **537**, 85 (2002)
20. J. T. Hinatsu, W. F. Graydon, F. R. Foulkes, *J.Appl.Electrochem*., **19**, 868 (1988)
21. J. Flis, H. W. Pickering, K. Osseo-Asare, *El.Acta*, **43**, 1921 (1998)
22. A.Hugot-Le Goff, J.Flis, N.Boucherit, S.Joiret, J.Wilinski, *J.Electrochem.Soc*, **137**, 2685 (1990)
23. C. Sarasola, T. Fernandez, Y. Jimenez, *El.Acta*, **33**, 1295 (1988)
24. S. Juanto, J. O. Zerbino, M. I. Miguez, J. R. Vilche, A.J.Arvia, *El.Acta*, **32**, 1743 (1987)
25. R. C. Salvarezza, D. V. Vasquez Moll, A. J. Arvia*, El.Acta*, **32**, 1421 (1987)
26. G. Paruthimal Kalaignan, V. S. Muralidharan, K. I. Vasu, *J.Appl.Electtrochem*., **17**, 1083 (1987)
27. A. Wieckowski, M. Veerashanmugamani, *J.Appl.Electrochem*., **15**, 675 (1985)
28. A. Wieckowski, E. Ghali, H. H. Le, *J.Electrochem.Soc*, **131**, 2024 (1984)
29. R. S. Shrebler Guzman, J. R. Vilche, A. J. Arvia, *J.Appl.Electrochem*., **11**, 551 (1981)